Bull. Mater. Sci., Vol. 26, No. 1, January 2003, pp. 131–135. © Indian Academy of Sciences.

Theoretical study of superconductivity in MgB_2 and its alloys

P P SINGH

Department of Physics, Indian Institute of Technology, Mumbai 400 076, India

Abstract. Using density-functional-based methods, we have studied the fully-relaxed, full-potential electronic structure of the newly discovered superconductor, MgB_2, and BeB_2, NaB_2 and AlB_2. Our results, described in terms of (i) total density of states (DOS) and (ii) the partial DOS around the Fermi energy, E_F, clearly show the importance of B *p*-electrons for superconductivity. For BeB_2 and NaB_2, our results indicate qualitative similarities but significant quantitative differences in their electronic structure due to differences in the number of valence electrons and the lattice constants *a* and *c*.

We have also studied $Mg_{1-x}M_xB_2$ ((M ≡ Al, Li or Zn) alloys using coherent-potential to describe disorder, Gaspari–Gyorffy approach to evaluate electron–phonon coupling, and Allen–Dynes equation to calculate the superconducting transition temperature, T_c. We find that in $Mg_{1-x}M_xB_2$ alloys (i) the way T_c changes depends on the location of the added/modified k-resolved states on the Fermi surface and (ii) the variation of T_c as a function of concentration is dictated by the B *p* DOS.

Keywords. Superconductivity; MgB_2; BeB_2; NaB_2; AlB_2.

1. Introduction

Since the discovery of superconductivity in MgB_2 (Nagamatsu *et al* 2001), the experimental (Bud'ko *et al* 2001; Buzea and Yamashita 2001; Hinks *et al* 2001; Nagamatsu *et al* 2001; Takahashi *et al* 2001; Yildirim *et al* 2001) and theoretical (An and Pickett 2001; Belaschenko *et al* 2001; Bohnen *et al* 2001; Choi *et al* 2001; Kong *et al* 2001; Kortus *et al* 2001; Liu *et al* 2001; Medvedeva *et al* 2001; Satta *et al* 2001; Singh *et al* 2001) efforts have greatly improved our understanding of the nature of interaction responsible for superconductivity (SC) in MgB_2. It has become clear that almost all facets of the phonon-mediated electron–electron interaction have a dramatic influence over the superconducting behaviour of MgB_2. For example, the electron–phonon matrix elements change considerably as one moves away from the cylindrical Fermi sheets along Γ to *A* (Choi *et al* 2001; Kong *et al* 2001), anharmonic effects (Liu *et al* 2001; Yildirim *et al* 2001) have to be included in the dynamical matrix (Choi *et al* 2001), and finally **k**-dependent fully anisotropic Eliashberg equations have to be solved (Choi *et al* 2001) for a complete and accurate description of the superconducting properties of MgB_2.

In order to understand SC in MgB_2, it is essential to have an accurate electronic structure description of the normal state MgB_2. It has also become clear that the boron layer and the two-dimensional σ band due to $p_{x,y}$ orbitals in that layer hold the key to SC in MgB_2. Thus an understanding of how the σ band and the $p_{x,y}$ orbitals respond to changes in the chemical environment, lattice constants etc could be quite useful in understanding SC in MgB_2 and in synthesizing new materials with MgB_2-like SC. Fortunately, these changes around B layer can be mimicked without destroying its two-dimensional character which is essential for SC. For example, the effects of removing one electron and adding one electron around the B layer can be studied by considering NaB_2 and AlB_2, respectively. Similarly, a study of BeB_2 (and NaB_2) will provide the effects of changing the lattice parameter, *c* and to a lesser extent, *a*. Thus an accurate and reliable systematic study of the electronic structure of MgB_2, BeB_2, NaB_2 and AlB_2, coupled with the experimental facts of SC in MgB_2 and no SC in AlB_2, can provide substantive clues about the nature of interaction responsible for SC.

Another avenue for learning more about the interaction responsible for superconductivity in MgB_2 is through the effects of alloying on it. As indicated above, a strong dependence of the superconducting properties of MgB_2 on different aspects of the interaction has opened up the possibility of dramatically modifying its superconducting behaviour by changing the interaction in various ways, and thereby learning more about the interaction itself. There have been several studies of changes in the SC properties of MgB_2 upon substitutions of various elements such as Be, Li, C, Al, Na, Zn, Zr, Fe, Co, Ni, and others (Buzea and Yamashita 2001; Moritomo *et al* 2001; Xiang *et al* 2001; Zhao *et al* 2001). The main effects of alloying are seen to be (i) a decrease in transition temperature, T_c, with increasing concentration of the alloying elements although the rate at which the T_c changes depends on the element being substituted, (ii) a slight increase in the T_c in case of Zn (Kazakov *et al* 2001; Moritomo *et al* 2001) substitution while for Si and Li the T_c remains essentially the same, (iii) persistence of superconductivity up to $x \sim 0{\cdot}7$ in $Mg_{1-x}Al_xB_2$ (Buzea and Yamashita 2001; Xiang *et al* 2001), (iv) a change in

crystal structure and the formation of a superstructure at $x = 0{\cdot}5$ in $Mg_{1-x}Al_xB_2$ (Xiang 2001), and (v) a change in the lattice parameters, a and c.

2. Results and discussion

In the following, we present the results of fully-relaxed, full-potential electronic structure calculations for MgB_2, BeB_2, NaB_2 and AlB_2 in $P6/mmm$ crystal structure, using density-functional-based methods. We analyse our results in terms of (i) density of states (DOS) and (ii) the partial DOS around the Fermi energy, E_F, in these systems. We also present the results of our calculations for $Mg_{1-x}M_xB_2$ (M ≡ Al, Li or Zn) alloys. We have used coherent–potential to describe disorder, Gaspari–Gyorffy approach to evaluate electron–phonon coupling, and Allen–Dynes equation to calculate the superconducting transition temperature, T_c, of these alloys.

For our calculations for ordered alloys, we have used ABINIT code (see URL http://www.pcpm.ucl.ac.be/abinit), based on pseudopotentials and planewaves, to optimize the lattice constants a and c of MgB_2, BeB_2, NaB_2 and AlB_2. In order to study the band-structure along symmetry directions and site- and symmetry-decomposed densities of states, we have calculated, self-consistently, the electronic structure of these compounds using our own full-potential program as well as LMTART package (Savrasov 1996) with the optimized lattice constants. For studying the charge density in a small energy window around E_F, we have used the Stuttgart TB LMTO package.

For $Mg_{1-x}Al_xB_2$, $Mg_{1-x}Li_xB_2$ and $Mg_{1-x}Zn_xB_2$ alloys, we have used Korringa–Kohn–Rostoker coherent-potential approximation (Faulkner 1982; Singh and Gonis 1994) in the atomic-sphere approximation (KKR–ASA CPA) method for taking into account the effects of disorder, Gaspari–Gyorffy formalism (Gaspari and Gyorffy 1972) for calculating the electron–phonon coupling constant, λ, and Allen–Dynes equation (Allen and Dynes 1975) for calculating T_c as a function of Al, Li and Zn concentrations, respectively. We have analysed our results in terms of the changes in the spectral function (Faulkner 1982) along Γ to A evaluated at E_F, and the total density of states (DOS), in particular, the changes in the B p contribution to the total DOS, as a function of concentration, x.

2.1 *Computational details*

Before describing our results in detail, we provide some of the computational details of our calculations. The structural relaxation was carried out by the molecular dynamics program ABINIT with Broyden–Fletcher–Goldfarb–Shanno minimization technique (see abinit) using Troullier–Martins pseudopotentials (Troullier and Martins 1991), 512 Monkhorst–Pack (Monkhorst and Pack 1976) **k**-points and Teter parametrization (see abinit) for the exchange–correlation. The kinetic energy cutoff for the plane waves was 110 Ry. The charge self-consistent full-potential LMTO calculations were carried out using 2k-panels with the generalized gradient approximation for exchange–correlation as given by Perdew *et al* (Perdew and Wang 1992; Perdew *et al* 1996) and 484 **k**-points in the irreducible wedge of the Brillouin zone. The basis set used consisted of s, p, d and f orbitals at the Mg site and s, p and d orbitals at the B site. The potential and the wavefunctions were expanded up to $l_{max} = 6$. The input to the tight-binding LMTO calculations, carried to charge self-consistency, was similar to that of the full-potential calculations except for using spherically symmetric potential and the space-filling atomic spheres.

The charge self-consistent electronic structure of $Mg_{1-x}Al_xB_2$, $Mg_{1-x}Li_xB_2$ and $Mg_{1-x}Zn_xB_2$ alloys as a function of x has been calculated using the KKR–ASA CPA method. We have used the CPA rather than a rigid-band model because CPA has been found to reliably describe the effects of disorder in metallic alloys (Faulkner 1982; Singh and Gonis 1994). We parametrized the exchange-correlation potential as suggested by Perdew–Wang (Perdew and Wang 1992; Perdew *et al* 1996) within the generalized gradient approximation. The Brillouin zone (BZ) integration was carried out using 1215 k-points in the irreducible part of the BZ. For DOS and spectral function calculations, we added a small imaginary component of 1 mRy and 2 mRy, respectively, to the energy and used 4900 **k**-points in the irreducible part of the BZ. The lattice constants for $Mg_{1-x}Al_xB_2$, $Mg_{1-x}Li_xB_2$ and $Mg_{1-x}Zn_xB_2$ alloys as a function of x were taken from experiments (Kazakov *et al* 2001; Xiang *et al* 2001; Zhao *et al* 2001). The Wigner–Seitz radii for Mg, Al and Zn were slightly larger than that of B. The sphere overlap which is crucial in ASA, was less than 10% and the maximum l used was $l_{max} = 3$.

The electron–phonon coupling constant, λ, was calculated using Gaspari–Gyorffy (Gaspari and Gyorffy 1972) formalism with the charge self-consistent potentials of $Mg_{1-x}Al_xB_2$, $Mg_{1-x}Li_xB_2$ and $Mg_{1-x}Zn_xB_2$ obtained with the KKR–ASA CPA method. Subsequently, the variation of T_c as a function of Al, Li and Zn concentrations was calculated using Allen–Dynes equation (Allen and Dynes 1975). The average values of phonon frequencies, ω_{ln}, for MgB_2 and AlB_2 were taken from Kong *et al* (2001) and Bohnen *et al* (2001), respectively. For intermediate concentrations, we took ω_{ln} to be the concentration-weighted average of MgB_2 and AlB_2. For $Mg_{1-x}Li_xB_2$ and $Mg_{1-x}Zn_xB_2$, we used the same value of ω_{ln} as that for MgB_2.

2.2 *Electronic structure*

We show in figure 1 the total density of states for BeB_2, NaB_2, MgB_2 and AlB_2 calculated using the ABINIT pro-

gram at the optimized lattice constants of these compounds as given in Singh (2001). The gross features of the DOS of the four compounds are similar if one takes into account the differences in the total number of valence electrons. The bottom of the band is the deepest for AlB_2 which has a total of nine valence electrons and shallowest for NaB_2 with only seven valence electrons. However, the isoelectronic structures, BeB_2 and MgB_2, show substantial differences in their DOS near the bottom of the band. This is due to the fact that the smaller c/a ratio leads to enhanced repulsion which pushes the s and p electrons at the Mg site downward and, at the same time, diminishes the DOS for B s and p electrons in the middle of the band. In the case of AlB_2, we find that the B p-band is completely inside E_F.

An important factor in determining the superconducting temperature in conventional superconductors is the DOS within an interval of $\pm \hbar\omega_D$ at E_F. In order to analyse our results in detail we have plotted in figure 2 the symmetry-decomposed DOS at the B site within a small energy interval around E_F. From the DOS for AlB_2, it is evident that it will not be superconducting, not at least in the same sense as that of MgB_2, because the bands with x and y symmetry are completely filled. According to our calculations as shown in figure 2, NaB_2 is likely to show SC with enhanced T_c.

2.3 *Superconducting transition temperature*

Based on our calculations, we find that in $Mg_{1-x}Al_xB_2$, $Mg_{1-x}Li_xB_2$ and $Mg_{1-x}Zn_xB_2$ alloys (i) the way T_c changes depends on the location of the added/modified **k**-resolved states on the Fermi surface, and (ii) the variation of T_c as a function of concentration is dictated by the B p contribution to the total DOS.

The main results of our calculations are shown in figure 3, where we have plotted the variation in T_c of $Mg_{1-x}Al_xB_2$, $Mg_{1-x}Li_xB_2$ and $Mg_{1-x}Zn_xB_2$ alloys as a function of concentration, x. The calculations were carried out as described earlier with the same value of $m^* = 0{\cdot}09$ for all the concentrations. The T_c for MgB_2 is equal to $\sim 30{\cdot}8$ K, which is consistent with the results of other works (Bohnen *et al* 2001; Kong *et al* 2001; Kortus *et al* 2001) with similar approximations. The corresponding λ is equal to 0·69. For $0 < x \leq 0{\cdot}3$, the T_c increases slightly for $Mg_{1-x}Li_xB_2$ and $Mg_{1-x}Zn_xB_2$, while it decreases substantially for $Mg_{1-x}Al_xB_2$, as is found experimentally (Buzea and Yamashita 2001; Xian *et al* 2001). Note that for $x = 0{\cdot}1$, our calculation shows $Mg_{1-x}Li_xB_2$ to have a T_c higher than that of $Mg_{1-x}Zn_xB_2$ by about 7 K (Kazakov *et al* 2001; Moritomo 2001; Zhao *et al* 2001). In figure 3 (right panel) we have shown the variation in T_c in $Mg_{1-x}Al_xB_2$ alloys as a function of concentration for

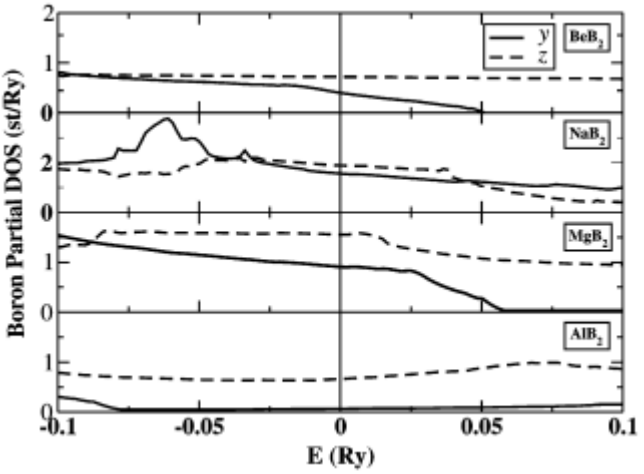

Figure 2. The partial B density of states around Fermi energy calculated at the optimized lattice constants using the full-potential LMTO method.

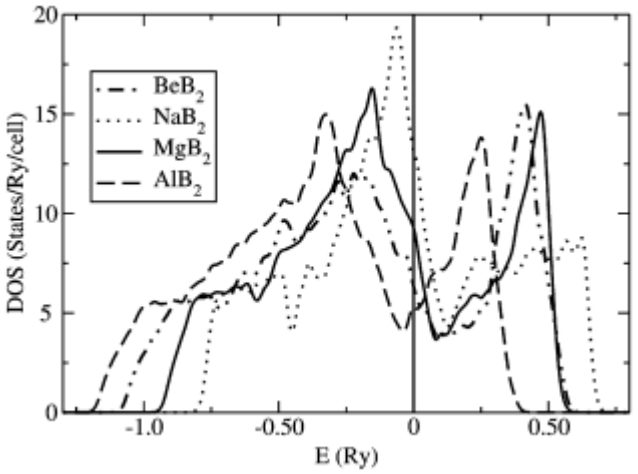

Figure 1. The total density of states calculated at the optimized lattice constants using the ABINIT program.

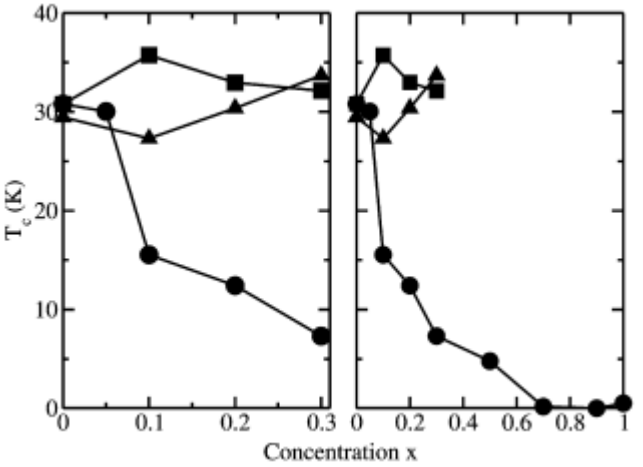

Figure 3. The calculated variation of T_c as a function of concentration x in $Mg_{1-x}Al_xB_2$ (filled circles), $Mg_{1-x}Li_xB_2$ (filled triangles) and $Mg_{1-x}Zn_xB_2$ (filled squares) alloys.

$0 \le x \le 1$. As a function of Al concentration, the T_c decreases rapidly from 30 K at $x = 0{\cdot}05$ to about 15 K at $x = 0{\cdot}1$. The T_c decreases slowly between $x = 0{\cdot}4$ and $0{\cdot}5$. At $x = 0{\cdot}7$, the T_c vanishes and remains essentially zero thereafter. The calculated variation in T_c, as shown in figure 3, is in very good qualitative agreement with the experiments (Buzea and Yamashita 2001).

In order to understand the variation of T_c in $Mg_{1-x}Al_xB_2$, $Mg_{1-x}Li_xB_2$ and $Mg_{1-x}Zn_xB_2$ alloys as a function of concentration, x, we have analysed our results in terms of the spectral functions, the contribution of boron p-electrons to the total DOS and the total DOS. In figures 4(a)–(c), we show the spectral functions along Γ to A direction evaluated at E_F in $Mg_{1-x}Al_xB_2$, $Mg_{1-x}Li_xB_2$ and $Mg_{1-x}Zn_xB_2$ alloys for $x = 0{\cdot}1$ (figure 4(a)), $x = 0{\cdot}3$ (figure 4(b)), and $x = 0{\cdot}6$–$1{\cdot}0$ (figure 4(c)). From figures 4(a)–(b), it is clear that the substitution of Al in MgB_2 leads to creation of more new states along Γ to A direction than the substitution of Zn or Li. Since the hole-like cylindrical Fermi sheet along Γ to A contributes much more to the electron–phonon coupling (Choi *et al* 2001), the creation of new electron states along Γ to A direction weakens considerably the overall coupling constant, $\boldsymbol{l}$, which, in turn, reduces the T_c more in $Mg_{1-x}Al_xB_2$ than in either $Mg_{1-x}Zn_xB_2$ or $Mg_{1-x}Li_xB_2$. Thus, in our opinion, the way T_c changes in MgB_2 upon alloying depends dramatically on the location of the added/modified **k**-resolved states on the Fermi surface.

Having explained the differences in behaviour of MgB_2 upon alloying with Al, Li and Zn, we now try to understand the changes in their properties as a function of concentration, x. In figures 5(a)–(b) we have shown the total DOS at E_F (figure 5(a)) and the B p contribution to the total DOS at E_F (figure 5(b)) in $Mg_{1-x}Al_xB_2$, $Mg_{1-x}Li_xB_2$ and $Mg_{1-x}Zn_xB_2$ alloys as a function of concentration, x. We find that as a function of concentration, the variation in T_c, as shown in figure 3, follows closely the behaviour of the total DOS at E_F and in particular the variation in B p contribution to the total DOS at E_F. It is also not surprising to see that the vanishing of superconductivity in $Mg_{1-x}Al_xB_2$ at $x \sim 0{\cdot}7$ coincides with a very small B p contribution to the total DOS.

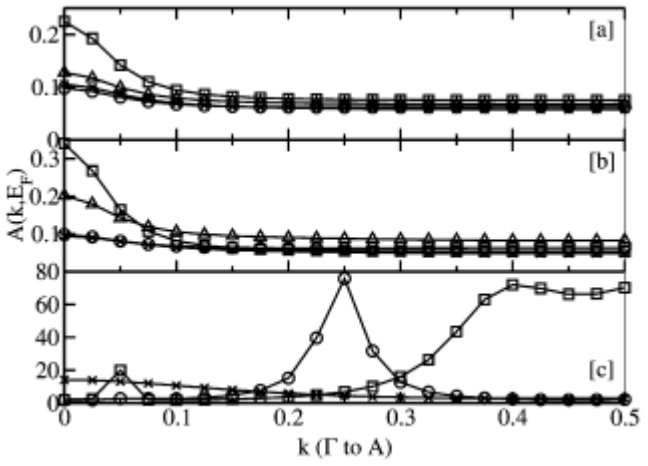

Figure 4. The calculated spectral function along Γ to A, evaluated at the Fermi energy, as a function of concentration, x, in $Mg_{1-x}Al_xB_2$, $Mg_{1-x}Li_xB_2$ and $Mg_{1-x}Zn_xB_2$ alloys. Figures (a) and (b) correspond to $x = 0{\cdot}1$ and $0{\cdot}3$, respectively and the symbols open circle, open square, × and open triangle correspond to MgB_2, $Mg_{1-x}Al_xB_2$, $Mg_{1-x}Li_xB_2$ and $Mg_{1-x}Zn_xB_2$ alloys, respectively. In figure (c) the symbols open circle, open square and × correspond to AlB_2, $Mg_{0{\cdot}1}Al_{0{\cdot}9}B_2$ and $Mg_{0{\cdot}4}Al_{0{\cdot}6}B_2$, respectively. For clarity, in figure (c) we have multiplied the spectral function of $Mg_{0{\cdot}4}Al_{0{\cdot}6}B_2$ by 100.

3. Conclusions

We have presented the results of our fully-relaxed, full-potential electronic structure calculations for BeB_2, NaB_2, MgB_2 and AlB_2 in *P*6/*mmm* crystal structure using density-functional-based methods. We have analysed our results in terms of the density of states, band-structure, and the DOS and the electronic charge density around E_F in these systems. For MgB_2, we find that the p-band of B is crucial for SC due to its proximity to E_F. For BeB_2 and NaB_2, our results indicate qualitative similarities but significant quantitative differences in the electronic structure due to differences in the number of valence electrons and the lattice constants.

We have also shown that in $Mg_{1-x}Al_xB_2$, $Mg_{1-x}Li_xB_2$ and $Mg_{1-x}Zn_xB_2$ alloys (i) the way T_c changes depends on the location of the added/modified **k**-resolved states on the Fermi surface, (ii) the variation of T_c as a function of concentration is dictated by the B p contribution to the total DOS at E_F.

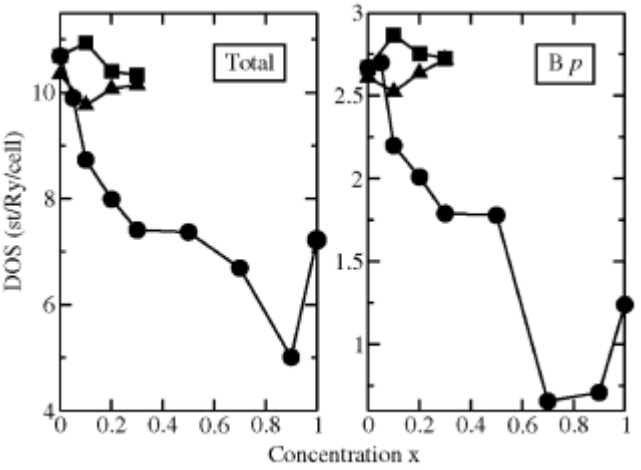

Figure 5. The calculated total density of states at the Fermi energy (left panel) and the B p contribution to the total DOS (right panel) in $Mg_{1-x}Al_xB_2$ (filled circles), $Mg_{1-x}Li_xB_2$ (filled triangles) and $Mg_{1-x}Zn_xB_2$ (filled squares) alloys.

References

Allen P B and Dynes R C 1975 *Phys. Rev.* **B12** 905
An M and Pickett W E 2001 *Phys. Rev. Lett.* **86** 4366
Belaschenko K D *et al* 2001 *Phys. Rev.* **B64** 092503
Bohnen K-P *et al* 2001 *Phys. Rev. Lett.* **86** 5771
Bud'ko S L *et al* 2001 *Phys. Rev. Lett.* **86** 1877
Buzea C and Yamashita T 2001 cond-mat/0108265; and references therein
Choi H J *et al* 2001 cond-mat/0111182 and cond-mat/0111183
Faulkner J S 1982 *Prog. Mater. Sci.* **27** 1; and references therein
Gaspari G D and Gyorffy B L 1972 *Phys. Rev. Lett.* **28** 801
Hinks D G *et al* 2001 *Nature* **411** 457
Kazakov S M *et al* 2001 cond-mat/0103350
Kong Y *et al* 2001 *Phys. Rev.* **B64** 020501
Kortus J *et al* 2001 *Phys. Rev. Lett.* **86** 4656
Liu A *et al* 2001 *Phys. Rev. Lett.* **87** 87005
Medvedeva N I *et al* 2001 *Phys. Rev.* **B64** 020502
Monkhorst H J and Pack J D 1976 *Phys. Rev.* **B13** 5188
Moritomo Y *et al* 2001 cond-mat/0104568
Nagamatsu J *et al* 2001 *Nature* **410** 63
Perdew J P and Wang Y 1992 *Phys. Rev.* **B45** 13244
Perdew J P *et al* 1996 *Phys. Rev. Lett.* **77** 3865
Savrasov S Y 1996 *Phys. Rev.* **B54** 16470
Satta G *et al* 2001 *Phys. Rev.* **B64** 104507
Singh P P and Gonis A 1994 *Phys. Rev.* **B49** 1642
Singh P P 2001 *Phys. Rev. Lett.* **87** 087004
Takahashi T *et al* 2001 *Phys. Rev. Lett.* **86** 4915
Troullier N and Martins J L 1991 *Phys. Rev.* **B43** 1993
Xiang J Y *et al* 2001 cond-mat/0104366
Yildirim T *et al* 2001 *Phys. Rev. Lett.* **86** 5771
Zhao Y G *et al* 2001 *Physica* **C361** 91